Automated tongue diagnosis on the smartphone and its applications

Min-Chun Hu[a,①], Kun-Chan Lan[b,a,①], Wen-Chieh Fang[c,①], Yu-chia Huang[d,①],
Tsung-Jung Ho[b,e,f,①], Chun-Pang Lin[f,①], Ming-Hsien Yeh[d], Paweeya Raknim[a],
Ying-Hsiu Lin[a], Ming-Hsun Cheng[a], Yi-Ting He[g], Kuo-Chih Tseng[g,h,*,①]

[a] *Department of Computer Science and Information Engineering, National Cheng Kung University, Tainan 701, Taiwan, ROC*
[b] *School of Chinese Medicine, China Medical University, Taichung 404, Taiwan, ROC*
[c] *Department of Geomatics, National Taiwan University, Taipei 10617, Taiwan, ROC*
[d] *Department of Chinese Medicine, Dalin Tzu Chi Hospital, Buddhist Tzu Chi Medical Foundation, Chiayi 62247, Taiwan, ROC*
[e] *Division of Chinese Medicine, China Medical University Beigang Hospital, Yunlin County 651, Taiwan, ROC*
[f] *Division of Chinese Medicine,Tainan Manicipal An-Nan Hospital -China Medical University, Tainan 709, Taiwan, ROC*
[g] *Department of Internal Medicine, Dalin Tzu Chi Hospital, Buddhist Tzu Chi Medical Foundation, Chiayi 622, Taiwan, ROC*
[h] *School of Medicine, Tzuchi University, Hualien, Taiwan, ROC*

* Corresponding author. School of Medicine, Tzuchi University, Hualien, Taiwan
Department of Internal Medicine, Dalin Tzu Chi Hospital, Buddhist Tzu Chi Medical Foundation, Chiayi, Taiwan
Address: No.2, Minsheng Rd., Dalin Township, Chiayi County 622, Taiwan
E-mail: tsengkuochih@gmail.com

① Min-Chun Hu, Kun-Chan Lan, Wen-Chieh Fang, Yu-chia Huang, Tsung-Jung Ho, Chun-Pang Lin, and Kuo-Chih Tseng contributed equally to this work.

Abstract

Tongue features are important objective basis for clinical diagnosis and treatment in both western medicine and Chinese medicine. The need for continuous monitoring of health conditions inspires us to develop an automatic tongue diagnosis system based on built-in sensors of smartphones. However, tongue images taken by smartphone are quite different in color due to various lighting conditions, and it consequently affects the diagnosis especially when we use the appearance of tongue fur to infer health conditions. In this paper, we captured paired tongue images with and without flash, and the color difference between the paired images is used to estimate the lighting condition based on the Support Vector Machine (SVM). The color correction matrices for three kinds of common lights (i.e., Fluorescent, Halogen and Incandescent) are pre-trained by using a ColorChecker-based method, and the corresponding pre-trained matrix for the estimated lighting is then applied to eliminate the effect of color distortion. We further use tongue fur detection as an example to discuss the effect of different model parameters and ColorCheckers for training the tongue color correction matrix under different lighting conditions. Finally, in order to demonstrate the potential use of our proposed system, we recruited 246 patients over a period of 2.5 years from a local hospital in Taiwan and examined the correlations between the captured tongue features and Alanine Aminotransferase (ALT) /Aspartate Aminotransferase (AST), which are important bio-markers for liver diseases. We found

that some tongue features have strong correlation with AST or ALT, which suggests the possible use of these tongue features captured on a smartphone to provide an early warning of liver diseases.

1. Introduction

Tongue features such as the tongue fur (or tongue coating) are important objective basis for clinical diagnosis and treatment in both western medicine and Chinese medicine. It is a clue for understanding a disease and can be referred to guide the determination of treatment based on different symptoms and signs. In western medicine, the underlining mechanism of tongue fur change have been investigated at the subcellular level and the gene level [8-11]. In traditional Chinese medicine (TCM), tongue diagnosis [1] is one of the most widely used diagnostic methods [2] since it reflects physiological conditions of a human body. Tongue diagnosis is a valuable reference for human health inspection. Inspection of the tongue can instantly clarify one's pathological problem, and it would be helpful for people seeking long-term health care to examine his/her tongue routinely.

Usually, several tongue features including tongue fur, tongue fissures, and tooth mark will be examined during the process of tongue diagnosis. However, the medical applications of traditional tongue diagnosis are limited by the fact that the clinical competence of tongue diagnosis is decided by the experience and knowledge of the practitioners. The diagnostic results based on the subjective analysis of the examiners may be unreliable and inconsistent. Therefore, it is important to have an objective and quantitative diagnostic process for tongue diagnosis.

To circumvent the subjective and qualitative problems of traditional tongue diagnosis, several computer aided tongue diagnosis systems have been proposed in the past decade [3–6]. For example, Zhang et al. [3] proposed a tongue diagnosis system that can identify five different diseases, including pulmonary heart disease, appendicitis, gastritis, pancreatitis, and bronchitis, based on Bayesian Networks with an accuracy about 75 %. However, to the best of our knowledge, the existing tongue diagnosis systems generally assume that the tongue images are taken in a well-controlled environment (e.g. with controlled lighting conditions, built-in color palettes for tongue color calibration, and fixed tongue position) and can be used only by the TCM doctors [7]. Fig. 1 shows a conventional tongue diagnosis system.

Fig. 1. A conventional tongue diagnosis system [49].

Recently, the need of extensive and continuous health monitoring has attracted increasing attention in both academia and industry. Extensive monitoring is beneficial to the quality of patient care, and continuous monitoring reduces the reaction time of sudden changes in patient's health condition. The large amount of collected data from each patient also allow doctors to predict future hazards of each patient more accurately, and to apply pre-emptive care accordingly. Given that mobile phone penetration in some countries is now almost 100 %, and most people carry their phones with them everywhere, smartphones provide a socially appropriate means of displaying timely information to the user and enable the physiological sensors to transmit measurements directly to health care providers. In addition, an increasing availability of built-in sensors (e.g. camera) for smartphone enables the measurement of the user's psychophysiology and environmental conditions. Together with associated mobile applications, it is possible to gather quality data for medical research or regular healthcare practice. Data can be gathered from the subjects unobtrusively for long periods of time, in a laboratory, as well as in a subject's daily living environment.

Based on aforementioned observations, we propose an automatic tongue diagnosis framework to analyze tongue images taken by the smartphone. Instead of using conventional tongue image capturing devices, we aim to let users take tongue images with their own smartphones no matter where they are. However, a main challenge arises in our application scenario: Even though we take photos of the same tongue with the same smartphone, images may look quite different in color due to various lighting conditions. The color distortion problem could reduce the accuracy of tongue feature detection and consequently affects tongue diagnosis. In order to solve this problem, we propose a method to detect tongue features under different lighting conditions. Our method includes

three main components: (1) A lighting condition classifier is trained based on the color distance of the tongue image pairs that are captured with/without flashlight. (2) The tongue image color correction matrices for different lighting conditions are trained using a ColorChecker-based correction method. (3) A tongue feature detector for images captured under the standard lighting condition is trained based on color features and SVM. When the user captures his/her tongue images via our smartphone-based tongue diagnosis system, the pretrained lighting condition classifier will be used to estimate the current lighting condition. Based on the estimated lighting condition, the corresponding color correction matrix will be used to transfer the tongue image color from specific lightings to standard lighting. Finally, the color-corrected tongue image is taken as the input to the tongue feature detector for making tongue diagnosis. Note that, in this paper, due to the space limitation, we use tongue fur detection as an example to illustrate our methodology.

In order to demonstrate the potential use of our proposed system, we recruited 246 patients over a period of 2.5 years from the health examination center and outpatients of Department of Gastroenterology and Hepatology of Dalin Tzuchi Hospital in Taiwan and examined the correlations between the captured tongue features and ALT/GPT [60] and AST/GOT [60] which are important bio-markers for liver diseases. We found that some tongue features have strong correlation with AST or ALT, which suggests the possible use of these tongue features captured on a smartphone to detect the early development of liver diseases.

The rest of this paper is organized as follows: Section 2 describes related works of tongue fur detection and tongue image color correction. Section 3 details our methodology of lighting condition estimation, tongue image color correction, and white fur detection. In section 4, we show the experimental results and further demonstrate, in section 5, the potential use of our tongue diagnosis system for non-invasive early detection of liver diseases. Finally, conclusion and future work are given in section 6.

2. Related works

2.1. Tongue Fur Detection

A tongue image shows the appearance of the tongue's substance that sometimes is coated with tongue fur. The appearance of tongue fur or tongue coating is one of the main tongue features which can be considered as a sign (biomarker) of internal changes and utilized to discover diseases and health state [8-11]. For example, formation of thick greasy tongue fur is closely related to papillae differentiations, the degree of papillae

proliferation, and the balance of proliferation, differentiation, and apoptosis of glossal epithelial cells [8]. Protein in the normal and pathological epithelial cells of tongue fur is associated with diseases of the digestive system [10] in western medicine. Moreover, the metabolites of tongue fur is related to the determination of TCM physical types like "Tanshi (痰濕)", "Qiyu (氣鬱)", etc. [13] in Chinese medicine. Thus, the detection of tongue fur plays an important role in computerized tongue diagnosis.

Most papers [12-18, 32, 34] extract or classify tongue fur with threshold-based methods. To be more precise, a tongue pixel is detected as tongue fur if its color values (e.g. RGB or HSI values) are larger than pre-defined thresholds or are in the pre-defined interval of color values. Instead of using pre-defined thresholds, a lot of researchers have proposed different learning methods to detect tongue fur [19-21, 23-31, 33], and Table 1 categorizes these methods. In this work, we use SVM to train the tongue fur detector based on RGB values. Our method is similar to the ones proposed in [24], [29] and [31]. However, these methods are applied to images captured under a controlled/standard lighting environment. When being applied to images captured by smartphone under various lightings, the accuracy of fur detection will drop drastically. Therefore, a proper color correction method to preprocess the captured tongue image is essential.

Table 1. Categories of different tongue fur detection methods.

		Only extract tongue fur (separate the body and fur)	Extract and classify tongue fur
Thresholding methods	RGB based	[18]	[32],[34]
	Non-RGB based	[14],[15],[16],[17]	[12],[13],[22],[32]
SVM	RGB based	[28]	[24],[29],[31]
	Grayscale		[23]
NN	RGB based		[30]
	Non-RGB based		[19],[30]
BN	RGB based		[27]
	Non-RGB based		[21], [23]
K-NN	RGB based		[25]
Fuzzy c-means	HSI	[26]	
Edge-Segmentation	RGB based	[18]	
	HSV	[20]	

2.2. Color Correction

Color correction has been extensively studied in the area of color science, and several correction algorithms have been proposed for different tasks. Tongue image color correction is an important issue in the field of

automatic tongue diagnosis, and a number of tongue image color correction methods have been investigated [3, 14, 35-43]. Existing research literature can be classified into four categories, i.e. methods based on simple image statistics, color temperature curve calibration, double exposure theory, and supervised learning [44]. Among the supervised learning methods, the polynomial regression-based correction method [45] is most commonly used because of its low computational complexity, which is important for online applications. Wang and Zhang [35] used the polynomial regression-based correction method for tongue image analysis and proved its effectiveness. The polynomial regression-based correction method requires a ColorChecker to be the reference for generating the color correction matrix. The ColorChecker contains a certain number of color patches as shown in Fig. 2. Wang and Zhang [36] further conducted a thorough and comprehensive study on the design of ColorChecker for more precise tongue color correction. Compared to the common Munsell ColorChecker, they proposed a space-based ColorChecker as shown in Fig. 2(b). However, the proper number and design of parameters for the polynomial regression-based correction method are not well studied. In this work, we also apply the polynomial regression-based method for tongue image color correction and deeply investigate into the design of model parameters.

(a)   (b)

Fig. 2. (a) The Munsell ColorChecker and (b) the ColorChecker used in [36].

3. Methodology

Color appearance of tongue images would be significantly affected by the environmental lighting condition, camera pose, or other camera settings such as white balance and focal length. This kind of color artifact consequently results in wrongly analysis of tongue features. Therefore, color correction, the procedure used to reveal the intrinsic color of the tongue under standard lighting condition, is essential for tongue image analysis. In previous studies of tongue image analysis, the tongues have to be captured in a certain device with fixed camera position, camera setting, and lighting condition [35, 36]. The constrained settings simplify the color correction procedure; however, our system works on smartphones and ordinary smartphone users usually do

not have a ColorChecker with them. Hence, we need to estimate the underlying lighting condition and use the corresponding pre-trained color correction matrix to transform the image from source lighting condition to standard lighting condition. Fig. 3 shows the overview of the proposed automatic tongue diagnosis system, which is composed of four main components, i.e. tongue photo taking guide, tongue image color correction, tongue region segmentation, and tongue fur analysis.
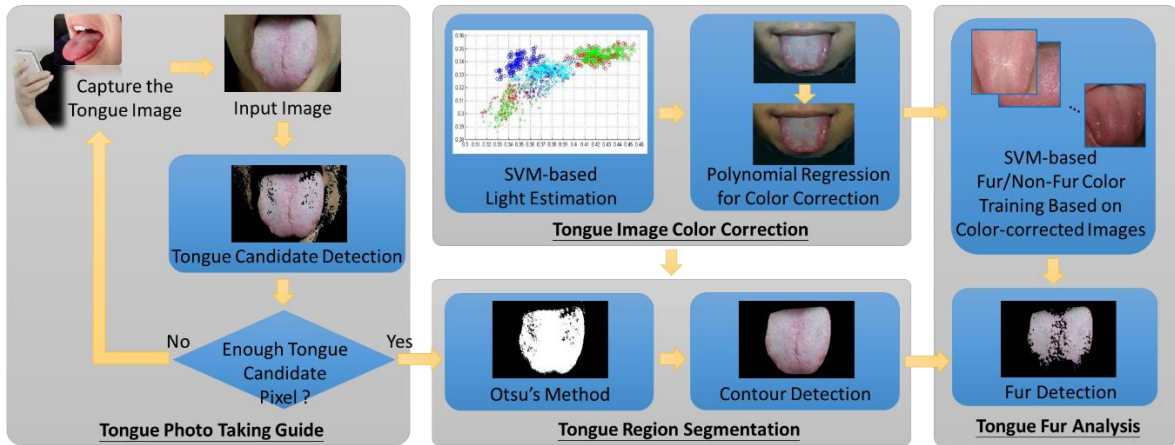

Fig. 3. the overview of the proposed automatic tongue diagnosis system.

3.1. Lighting Condition Estimation

Lighting Condition Estimation is a challenging and unsolved problem. In this work, we propose a novel lighting estimation method based on analyzing the CIE xyY color information of photos taken with/without flash. The CIE XYZ color space (also known as the CIE 1931 color space) is the first attempt to produce a color space based on measurements of human color perception and also the basis for almost all other color spaces [50]. Since the human eye has three types of color sensors that respond to different ranges of wavelengths, a full plot of all visible colors is in a three-dimensional space. However, the concept of color can be divided into two parts: brightness and chromaticity. The CIE XYZ color space was deliberately designed so that the Y parameter was a measure of the brightness or luminance of a color; the chromaticity of a color was then specified by the two values x and y, which are functions of all three tristimulus values X, Y, and Z. The derived color space specified by x, y, and Y is known as the CIE xyY color space and is widely used to specify colors in practical applications. To simplify the lighting estimation problem, we try to classify the current lighting into one of common lights (Table 2 shows the color temperatures of common lights). Note that only the chromaticity

values are considered to estimate the lighting because brightness is not related to color temperature. Fig. 4 shows the CIE 1931 xy chromaticity diagram [52].

Table 2. The color temperatures of common lights.

Light Source	Color Temperature
Fluorescent tube	6900K
Standard D65 fluorescent tube (our Ground truth)	6500K
Incandescent bulb	2800K
Halogen lamp	2700K
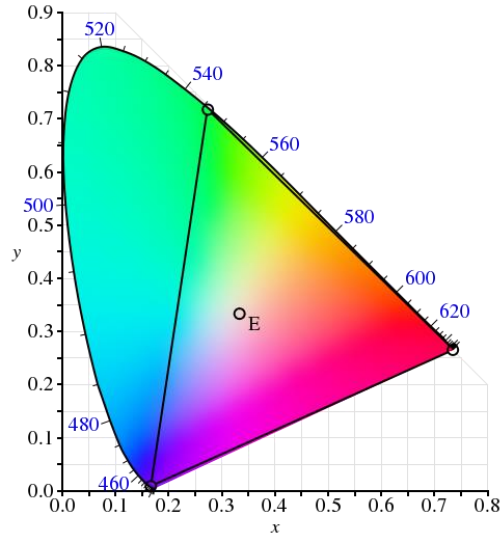
Fig. 4. CIE 1931 xy chromaticity diagram [52].

Given two tongue image patches $P1$ and $P2$, $C_1 = (x_1, y_1)$ and $C_2 = (x_2, y_2)$ denote the corresponding average chromaticity color inside the patch $P1$ and $P2$ respectively in the CIE xyY color space when the two patches are captured under the light L. $C_1' = (x_1', y_1')$ and $C_2' = (x_2', y_2')$ denote the chromaticity colors when the two patches are captured with the camera's flash under the same light L. Besides, in this paper, a pair of the tongue images capturing the same tongue with and without flash (under the same light L) are called a tongue image pair.

Our hypothesis

As shown in Fig. 5, using flash to recapture two tongue patches under the same light would just like imposing an intensity value to each channel of the original color. That is,

$$x_1' - x_1 \approx x_2' - x_2 \approx f_x,$$
$$y_1' - y_1 \approx y_2' - y_2 \approx f_y. \tag{1}$$

In other words, the color distance vectors of tongue image pairs captured under the same light would be similar even though the tongues are from the different people (as shown in Fig. 6). Moreover, the imposed intensity values (f_x, f_y) would be various under different lights even though the tongues are from the same user (as shown in Fig. 7). Hence, we can use the color distance vector between images captured with/without flash, i.e. (f_x, f_y), to estimate the current light.
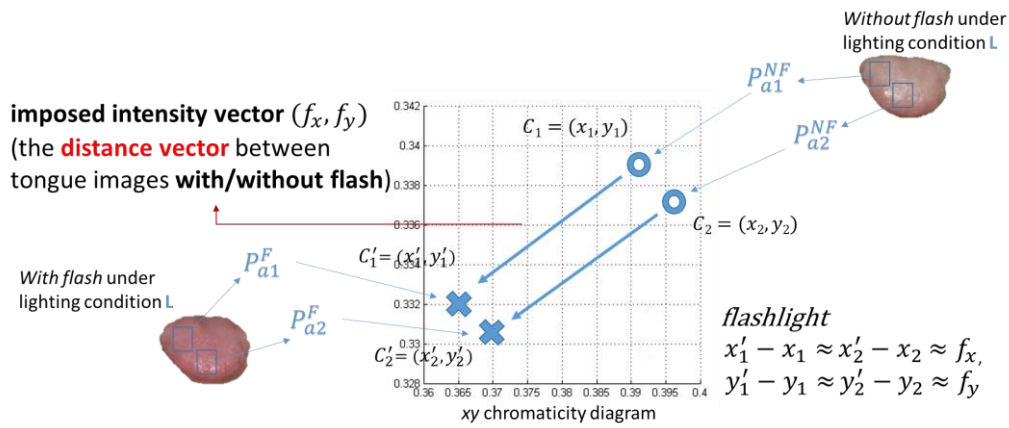
Fig. 5. Concept of the imposed intensity vector (f_x, f_y).
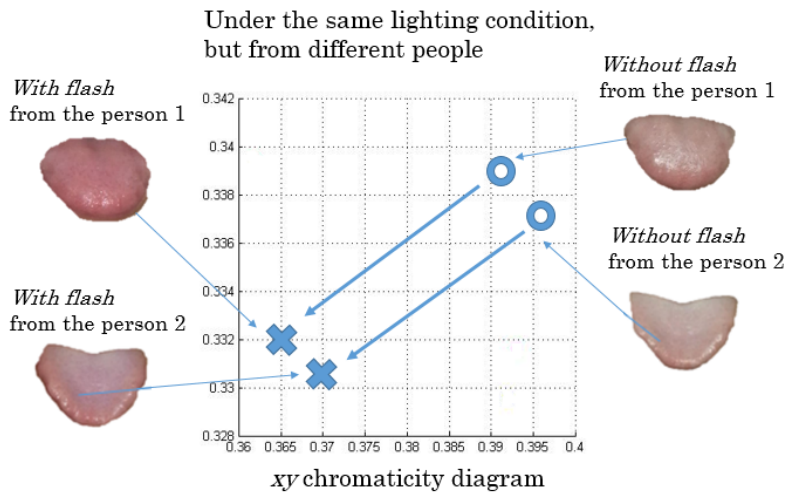
Fig. 6. The color distance vectors of different people under the same light.
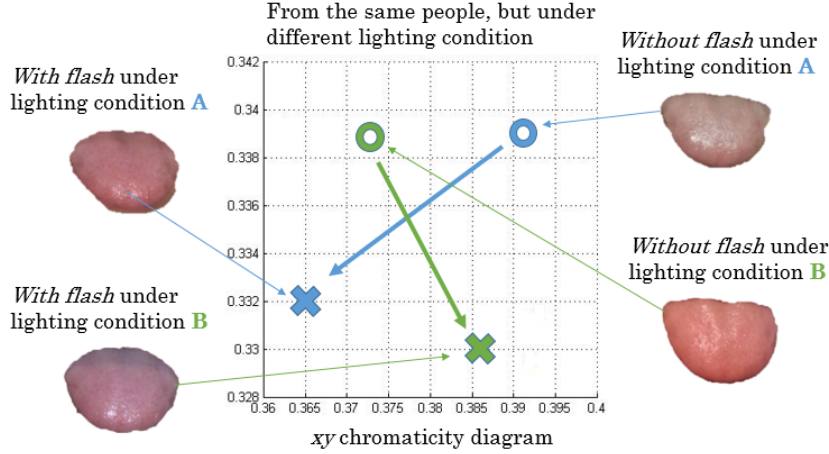
Fig. 7. The distance vectors of the same tongue under different lights.

In order to prove our hypothesis mentioned above, we collect 170 tongue image pairs (with/without flash) of different people. These images are captured under various lights and transformed from sRGB to CIE xyY color space to obtain the (x, y) chromaticity coordinates for each pixel inside the tongue region [48]. For each image, the mean coordinate (x_{mean}, y_{mean}) of all tongue color pixels is calculated and regarded as the color center of the tongue image. We plot color centers of all images in the (x, y) color coordinate to form a tongue color distribution in xy chromaticity diagram, as shown in Fig. 8. We capture N_k tongue image pairs (with/without flash) of different people under each light L_k. As shown in Fig. 9, different colors indicate that the images are taken under different lights L_k's, and each cross(X) and circle(O) sign represents the image is captured with and without flash, respectively. $(C_i^F(L_k), C_i^{NF}(L_k))$ indicate the color centers of the ith image pair that are captured under light L_k. For each lighting condition, each UP-POINTING TRIANGLE is the mean color of the tongue images captured without flash, and each DOWN-POINTING TRIANGLE is the mean color of the tongue images captured with flash.
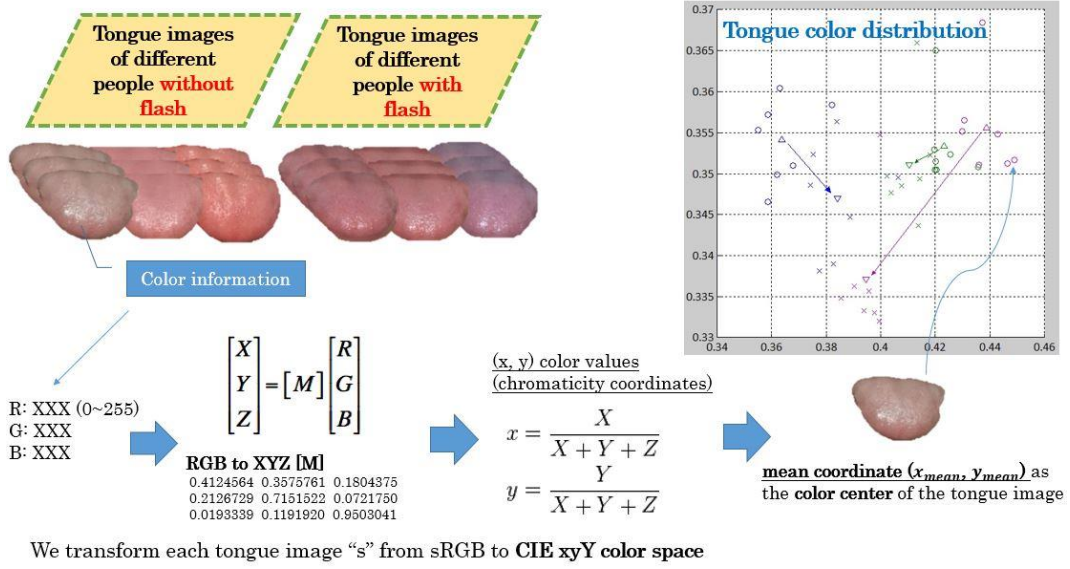
We transform each tongue image "s" from sRGB to **CIE xyY color space**

Within the figure, the following text appears:

Tongue images of different people without flash

Tongue images of different people with flash

Color information

Tongue color distribution

R: XXX (0~255)
G: XXX
B: XXX

$$\begin{bmatrix} X \\ Y \\ Z \end{bmatrix} = [M] \begin{bmatrix} R \\ G \\ B \end{bmatrix}$$

RGB to XYZ [M]
0.4124564 0.3575761 0.1804375
0.2126729 0.7151522 0.0721750
0.0193339 0.1191920 0.9503041

(x, y) color values
(chromaticity coordinates)

$$x = \frac{X}{X+Y+Z}$$

$$y = \frac{Y}{X+Y+Z}$$

mean coordinate (x_{mean}, y_{mean}) as the **color center** of the tongue image

Fig. 8. Process of generating the tongue color distribution.
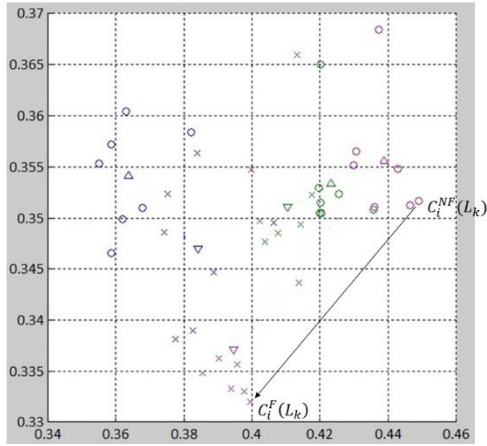
Fig. 9. Tongue color distribution in *xy* chromaticity diagram.

(a)   (b)
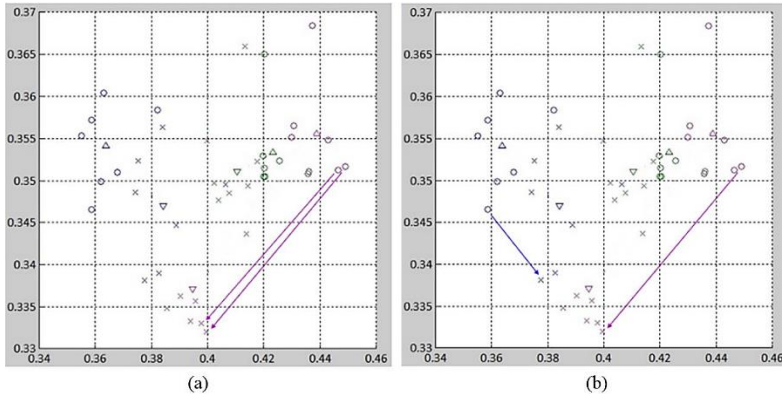
Fig. 10. Proof of our hypothesis

As indicated in Fig. 10 (a), we observe that the distance vector $C_i^F(L_k) - C_i^{NF}(L_k)$ would be similar under the same light L_k even for different tongues. On the other hand, even for the same tongue the distance vector $C_i^F(L_k) - C_i^{NF}(L_k)$ would be quite different if the tongue images are taken under different lights, as shown in Fig. 10 (b). Moreover, the quantitative analysis of distance distortion for each kind of light is provided in the experiment (cf. Section 4.1) . These results preliminarily verify our hypothesis, and we further apply LIBSVM (Multi-class classification and probability output via error-correcting codes) [47] to train a light estimation classifier based on the distance vector $C_i^F(L_k) - C_i^{NF}(L_k)$. When the user uses the smartphone to capture the tongue image, our system will automatically capture two images (one with flashlight and one without flashlight) and use them to estimate the lighting condition based on the pre-trained SVM classifier.

3.2. Tongue Image Color Correction

We apply the polynomial regression method for color correction and its concept is illustrated in Fig. 11. For each color patch i, the color value when it is captured under a source lighting is denoted as (R_i, G_i, B_i), and the corresponding color value when i is captured by the same camera under the target/standard lighting condition is denoted as (SR_i, SG_i, SB_i). The relation between (R_i, G_i, B_i) and (SR_i, SG_i, SB_i) can be considered as a polynomial transformation, that is

$$\begin{cases} SR_i = a_{11}R_i + a_{12}G_i + a_{13}B_i + \cdots \\ SG_i = a_{21}R_i + a_{22}G_i + a_{23}B_i + \cdots \\ SB_i = a_{31}R_i + a_{32}G_i + a_{33}B_i + \cdots \end{cases} \qquad (2.1)$$

The above equation can be rewritten in the matrix form:

$$\underbrace{\begin{pmatrix} SR_1 & SR_2 & \dots & SR_{24} \\ SG_1 & SG_2 & \dots & SG_{24} \\ SB_1 & SB_2 & \dots & SB_{24} \end{pmatrix}}_{S_{3\times24}} = \underbrace{\begin{pmatrix} a_{11} & a_{12} & a_{13} \\ a_{21} & a_{22} & a_{23} \\ a_{31} & a_{32} & a_{33} \end{pmatrix}}_{A_{3\times3}} \underbrace{\begin{pmatrix} R_1 & R_2 & \dots & R_{24} \\ G_1 & G_2 & \dots & G_{24} \\ B_1 & B_2 & \dots & B_{24} \end{pmatrix}}_{X_{3\times24}}, \qquad (2.2)$$

where A is the coefficient matrix, i.e. the color correction matrix, and can be estimated by using the least-square regression method.
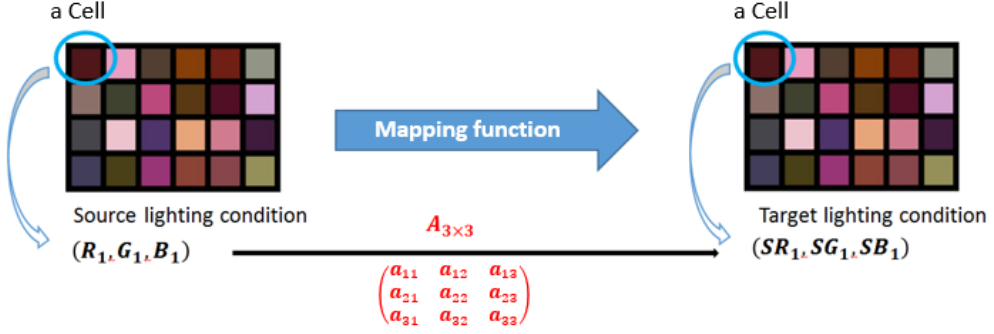
Fig. 11. The concept of the polynomial regression-based color correction method.

The performance of the polynomial regression-based color correction method would be affected by two factors: (1) The design of the ColorChecker, including the number of patches and the selected colors. (2) The design of the model parameters. To be more precise, Eq.(2.1) and Eq.(2.2) only use the first degree terms to model the polynomial transformation. However, taking more polynomial terms into consideration might result in better color correction accuracy. For example, Eq.(3) considers not only the first degree terms but also some second degree terms:

$$\begin{cases} SR_i = a_{11}R_i + a_{12}G_i + a_{13}B_i + a_{14}R_i^2 + a_{15}G_i^2 + a_{16}B_i^2 \\ SG_i = a_{21}R_i + a_{22}G_i + a_{23}B_i + a_{24}R_i^2 + a_{25}G_i^2 + a_{26}B_i^2 \\ SB_i = a_{31}R_i + a_{32}G_i + a_{33}B_i + a_{34}R_i^2 + a_{35}G_i^2 + a_{36}B_i^2 \end{cases} \quad . \tag{3}$$

The above equation can be rewritten in the matrix form:

$$\underbrace{\begin{pmatrix} SR_1 & SR_2 & ... & SR_{24} \\ SG_1 & SG_2 & ... & SG_{24} \\ SB_1 & SB_2 & ... & SB_{24} \end{pmatrix}}_{S_{3\times24}} = \underbrace{\begin{pmatrix} a_{11} & a_{12} & \cdots & a_{16} \\ a_{21} & a_{22} & \cdots & a_{26} \\ a_{31} & a_{32} & \cdots & a_{36} \end{pmatrix}}_{A_{3\times6}} \underbrace{\begin{pmatrix} R_1 & R_2 & ... & R_{24} \\ G_1 & G_2 & ... & G_{24} \\ B_1 & B_2 & ... & B_{24} \\ R_1^2 & R_2^2 & ... & R_{24}^2 \\ G_1^2 & G_2^2 & ... & G_{24}^2 \\ B_1^2 & B_2^2 & ... & B_{24}^2 \end{pmatrix}}_{X_{6\times24}} \tag{4}$$

In Section 4.2, we will show the comparison of using different polynomial models to correct the tongue images taken under different lights.

3.3. Tongue Feature Detection

After estimating the current lighting condition and applying the corresponding color correction matrix, we further detect tongue features in the color corrected tongue image. In this paper, as an example, a white fur detection model for images taken under standard lighting condition is trained based on SVM in advance. We

gathered tongue images taken under standard lighting condition and manually label the white fur and non-white-fur regions. RGB values of each pixel are utilized as the input features for training the SVM model.

4. Experimental Results

We evaluate the proposed methodology in terms of three parts: lighting condition estimation, tongue image color correction and white fur detection. To obtain the ground truth of tongue images captured under standard lighting condition, we built a simulator (a tongue image imaging system) and used it to collect tongue image pairs. The whole imaging system consists of a darkroom box, specific illuminants and a smartphone.

In our experiment, Samsung Galaxy S3 smartphone is used as the imaging device and tongue images captured in standard D65 illuminant are taken as the ground truth for color correction. The detailed specification of our simulator is described as follows.

Darkroom Box：
  • Box size：70(cm)*55(cm)*62(cm)
  • Distance between the smartphone and the target tongue：28cm
Illuminant：(color temperature)
  • Standard D65 fluorescent tube (our Ground truth)：6500K
  • Fluorescent tube：6900K
  • Halogen lamp：2700K
  • Incandescent bulb：2800K
Smartphone (Imaging device)：Samsung Galaxy S3
  • ISO：400
  • Metering mode：spot metering
 • White balance：default
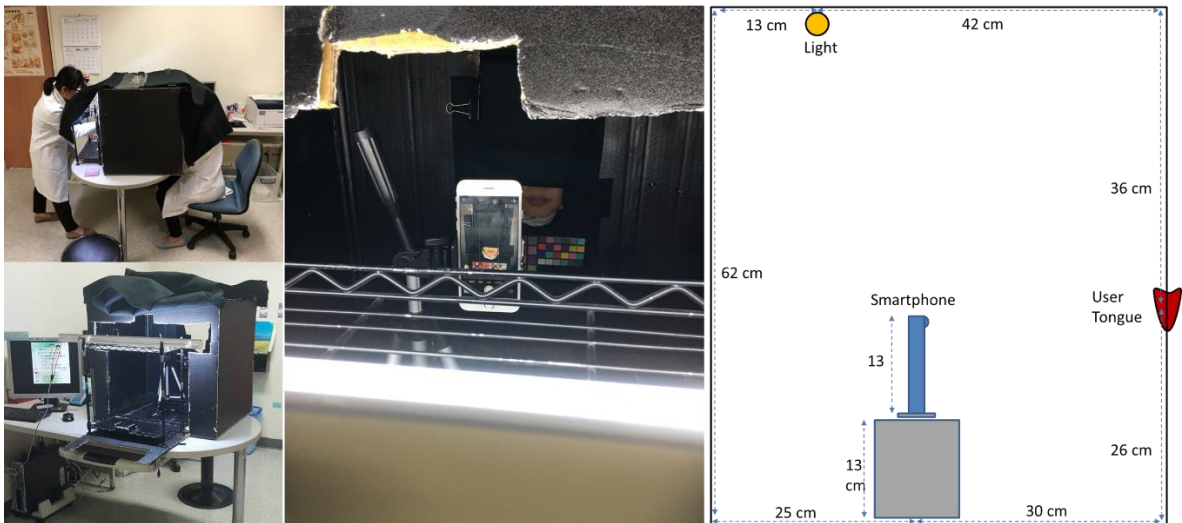
Fig. 12. Images of the darkroom and the specification of the camera/tongue position

We collected about 170 tongue image pairs (with/without flash) per light. 20 subjects in the age between 20 and 30 years old were recruited to take tongue photos under the four kinds of illuminants.

4.1. Evaluation of Lighting Condition Estimation

We first verify our hypothesis as described in section 3-1. All of the collected tongue images of different people are captured under four various lights with and without flash, and the corresponding tongue color distribution in the xy color coordinate is shown in Fig. 13. The distance vectors of tongue image pairs are similar when they are taken under the same lights and are different when they are taken under different lights. For each kind of light, the mean and standard deviation of the tongue color captured with/without flash and the distance vector are also reported in Fig. 13.
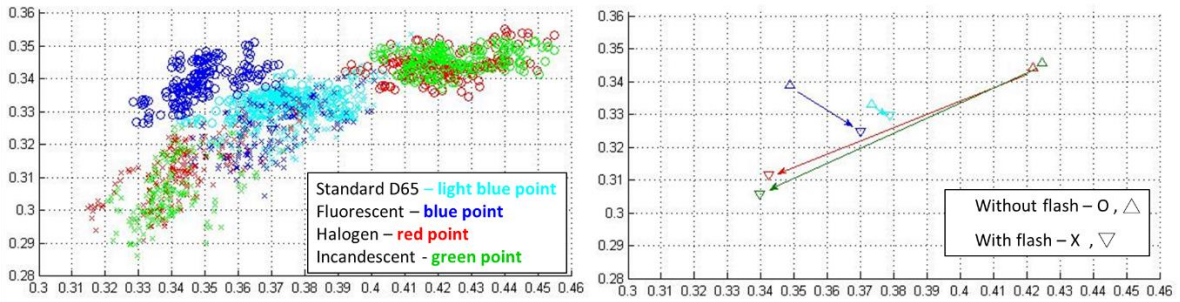
	Without Flash (x,y)		With Flash (x,y)		Distance Vector (x,y)	
	Mean	SD	Mean	SD	Mean	SD
D65	(0.373, 0.333)	(0.012, 0.003)	(0.379, 0.330)	(0.012, 0.007)	(0.006, -0.003)	(0.005, 0.006)
Fluorescent	(0.349,0.340)	(0.010, 0.006)	(0.370,0.325)	(0.013, 0.008)	(0.021, -0.014)	(0.007, 0.005)
Halogen	(0.422, 0.344)	(0.013, 0.004)	(0.342, 0.312)	(0.012, 0.009)	(-0.079,-0.033)	(0.013, 0.007)
Incandescent	(0.425, 0.346)	(0.013, 0.003)	(0.340, 0.306)	(0.010, 0.009)	(-0.095, -0.040)	(0.012, 0.008)

Fig. 13. Tongue color distribution of all collected tongue image pairs (the left image) and the mean distance vector of all images for each light (the right image). For each kind of light, the mean and standard deviation of the tongue color captured with/without flash and the distance vector are reported.

We use the five-fold cross-validation method to evaluate the prediction accuracy of the lighting estimation model, and Table 3 shows the results. The average accuracy of lighting estimation is 91.19%. The color distribution for Halogen (red point) is similar to that for Incandescent (Magenta point) and therefore the estimation accuracy for these two illuminants are only around 80%. We further assume that the tongue color distribution of paired images are similar under lights with similar Color Temperature, and their color correction matrix should be similar too. To verify this, we applied the same color correction matrix (either the one pre-

trained for Halogen or the one pre-trained for Incandescent) to correct tongue images captured under Halogen or Incandescent. Table 4 shows that the overlap rate (please see the definition in Section 4.2) between the images corrected with the pre-trained halogen correction matrix and the pre-trained incandescent correction matrix is high, which implies that wrongly classifying the lights of similar Color Temperature would not significantly affect the result of color correction.

Table 3. Prediction accuracy of our lighting estimation model.

	Number of Training data	Number of Testing data	D65 Accuracy	Flu. Accuracy	Hal. Accuracy	Inc. Accuracy	Total Accuracy
Run 1	146	580	100% (39/39)	100% (35/35)	71.43% (25/35)	86.49% (32/37)	89.73% (131/146)
Run 2	145	581	100% (39/39)	100% (35/35)	79.41% (27/34)	89.19% (33/37)	92.4138% (134/145)
Run 3	145	581	100% (40/40)	100% (34/34)	79.41% (27/34)	86.49% (32/37)	91.72% (133/145)
Run 4	145	581	100% (39/39)	100% (35/35)	79.41% (27/34)	89.19% (33/37)	92.4138% (134/145)
Run 5	145	581	100% (40/40)	100% (34/34)	85.29% (29/34)	70.59% (24/34)	89.66% (130/145)
Average Accuracy			100%	100%	79%	84.39%	91.19%

Table 4. Cross correction result for images taken under halogen and incandescent by using the pre-trained correction matrix for halogen and incandescent.

	Hal. tongue image	Inc. tongue image
Corrected by hal. correction matrix		
Corrected by Inc. correction matrix		
Overlap rate between them	0.8808	0.9301

4.2. Evaluation of Tongue Image Color Correction

To evaluate the performance of color correction on tongue images, we compare the color distributions of the tongue image taken under standard light and the corrected tongue image in the xy chromatic diagram. The overlap rate of two distributions is illustrated in Fig. 14 [35]. *A* is the area of "standard tongue image" in the color distribution space, B is the overlapping area of "standard tongue image" and "original/corrected tongue image" in the color distribution space. The overlap rate is defined as B/A, and we observe whether the overlap rate is increased after color correction.
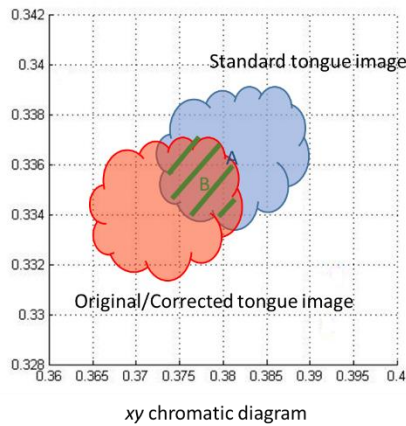
Fig. 14. The definition of overlap ratio.

In contrast to the polynomial transformation model used by Wang and Zhang [35], we further investigate the effect of using different polynomial models. Seven polynomial models considering different first degree and second degree terms are compared in our experiment:

- M1：[R,G,B] (used in [35, 36])
- M2：[R,G,B,1]
- M3：[R,G,B,RGB,1]
- M4：[R,G,B,R^2, G^2, B^2,RG,RB,GB]
- M5：[R,G,B,R^2, G^2, B^2,RG,RB,GB,RGB,1]
- M6：[R,G,B,R^2, G^2, B^2,RG,RB,GB,1]
- M7：[R,G,B,R^2, G^2, B^2, RGB,1]

We trained the color correction matrices for these 7 polynomial models and test all tongue images captured under Fluorescent, Halogen or Incandescent light with the corresponding pre-trained color correction matrices. The performance is evaluated based on the overlap rate and Fig. 15~Fig. 17 show the comparisons of using

different models for images captured under Fluorescent, Halogen and Incandescent light, respectively. The results show that although the M1 polynomial model used in [35, 36] performs well for images taken under Fluorescent light, it fails to correct images taken under the Halogen and Incandescent lights. Instead, the M2 polynomial model performs better than others under the Halogen and Incandescent lights. Fig. 18 shows an example result of using the M2 polynomial model to correct two images taken under the Halogen light and Incandescent light, respectively.
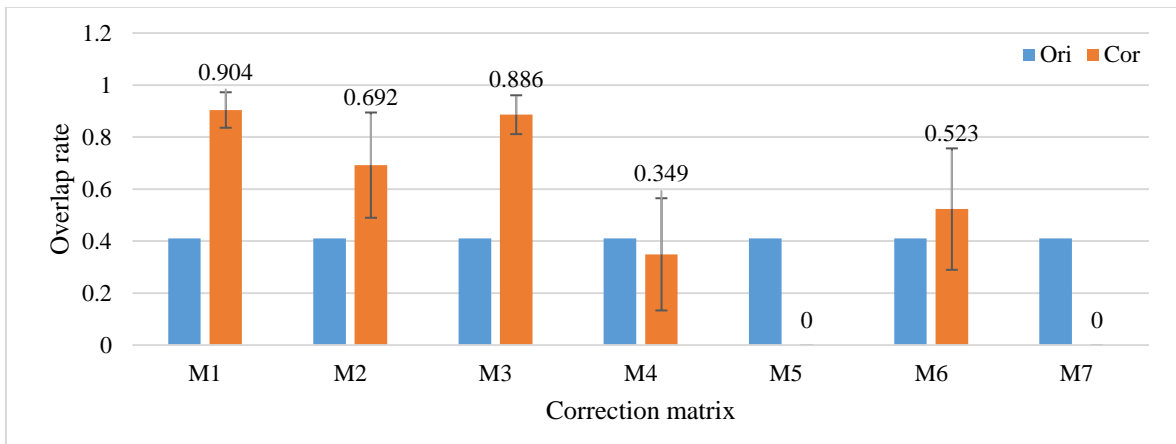
Fig. 15. Mean and Standard deviation of overlap rate for tongue images taken under the *Fluorescent light* by using 7 different polynomial transformation models for color correction.
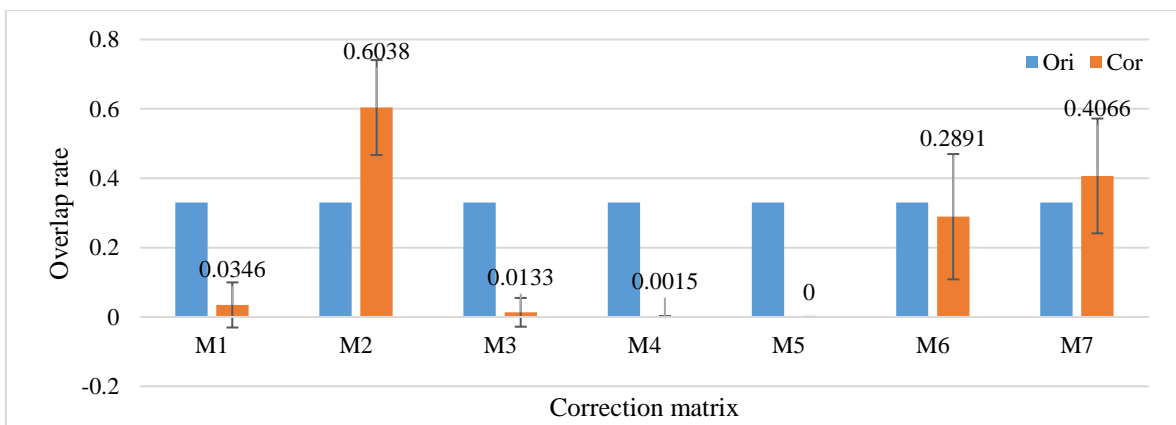
Fig. 16. Mean and Standard deviation of overlap rate for tongue images taken under the *Halogen light* by using 7 different polynomial transformation models for color correction.
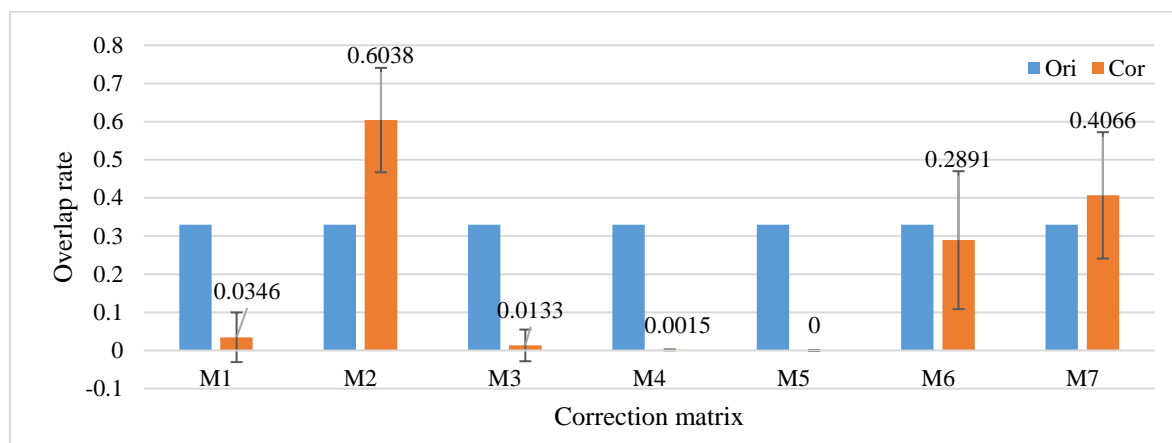
Fig. 17. Mean and Standard deviation of overlap rate for tongue images taken under the *Incandescent light* by using 7 different polynomial transformation models for color correction.
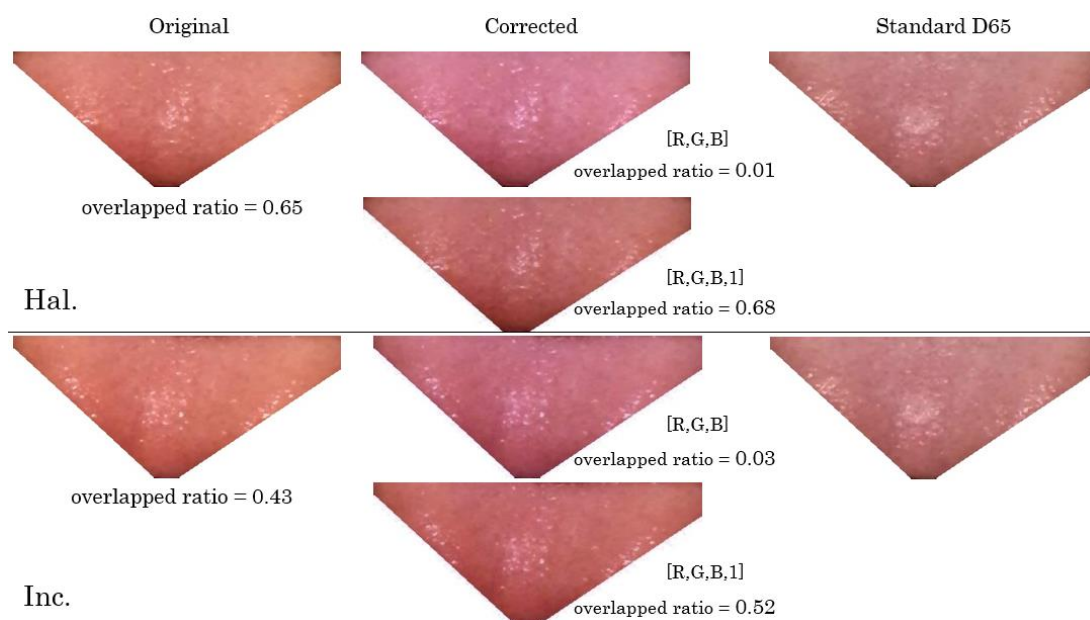

Fig. 18. Color correction results (overlapped ration) for Hal. and Inc. lighting with the combination of polynomial terms [R,G,B,1].

4.3. Evaluation of White Fur Detection

Due to the space limitation, in this paper we mainly focus on the detection of white fur, which is one of the most important tongue features. We compare the white fur detection results between the tongue images with and without color correction. Table 5 shows that our color correction method is effective for white fur detection since the detected fur region is almost the same as the ground truth after applying color correction. Without

color correction, white fur cannot be accurately detected for tongue images captured under the Halogen and Incandescent lights. Table 6 shows that tongue features like white fur can be identified if the overlap rate between the original tongue image and the corrected tongue image exceeds 60%, even if they are captured under quite different lighting conditions such as under the Halogen and Incandescent lights. Table 7 shows the confusion matrix of white fur detection results for all tongue images captured under the Fluorescent, Halogen and Incandescent lights.

Table 5. White fur detection results for tongue images captured under different lights with/without color correction

Standard D65 (Ground truth)	Correction	Overlapped ratio		
		Flu.	Hal.	Inc.
	Before Correction	0.64	0.22	0.18
	After Correction	0.98	0.65	0.63

Table 6. White fur detection results for three different tongue images captured under the Halogen and Incandescent lights with/without color correction.
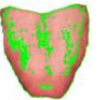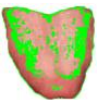
Standard D65 (Ground truth)	Overlapped ratio		Standard D65 (Ground truth)	Overlapped ratio		Standard D65 (Ground truth)	Overlapped ratio	
	Hal.	Inc.		Hal.	Inc.		Hal.	Inc.
Before Correction	0.22	0.18		0.38	0.24		0.29	0.22
After Correction	0.65	0.63		0.74	0.69		0.72	0.68

Table 7. Confusion matrix of white fur detection results of all tongue images captured under the Fluorescent, Halogen and Incandescent lights.

True condition\Predicted condition	Predicted Condition positive (with white fur)	Predicted Condition negative (without white fur)	
Condition positive (with white fur)	(TP) 66	(FN) 2	Recall(TP/TP+FN)= 0.97
Condition negative (without white fur)	(FP) 6	(TN) 6	
Flu.	Precision(TP/TP+FP) = 0.92		Accuracy(TP+TN/Total) = 0.9
Condition positive (with white fur)	(TP) 63	(FN) 5	Recall(TP/TP+FN)= 0.93
Condition negative (without white fur)	(FP) 5	(TN) 7	
Hal.	Precision(TP/TP+FP) = 0.93		Accuracy(TP+TN/Total) = 0.875
Condition positive (with white fur)	(TP) 61	(FN) 7	Recall(TP/TP+FN) = 0.9
Condition negative (without white fur)	(FP) 2	(TN) 10	
Inc.	Precision(TP/TP+FP) = 0.97		Accuracy(TP+TN/Total) = 0.8875

5. Application on Early Warning of Liver Disease

Chronic viral hepatitis B and C, and related liver diseases (liver cirrhosis and HCC) are major health problems in Taiwan [53]. Not only in Taiwan, primary liver cancer is the sixth most frequent cancer globally, and the second leading cause of cancer death [54]. Higher rates of liver cancer occur where hepatitis B and C are common, including East-Asia and sub-Sahar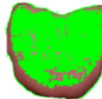an Africa [55]. Most people infected with the hepatitis B and C virus have no or mild symptoms, so they might not know they are infected. Over time, the liver inflammation caused by hepatitis B and C results in serious damage to the liver, like cirrhosis. People with cirrhosis have an increasing risk of developing liver cancer which, again, often causes no symptoms of its own when it first develops. Therefore, it may be too late when patients discover they have the cancer, and then the only possible solution left is the liver transplant. While successful treatment of hepatitis B and C prior to the development of cirrhosis prevents all these complications, people may not know they are infected with hepatitis B or C until it is too late, since the symptoms are not clear and might be neglected. When the viruses are not treated, the patient may proceed to have cirrhosis or liver cancer, which is usually irreversible. A common procedure to monitor the liver situation of hepatitis B or C carriers is to have a test every six months. Patients with cirrhosis need to have an ultrasound scanning every three months to check for signs of cancer. Most of the procedures above are effective but need to be done in the hospital, and some of these tests may cause damage to the body. Finally, due to the restriction of insurance policy, these procedures cannot be done very often.

Recently, the need for continuous monitoring of health conditions have attracted increasing attention in both academia and industry. Such an extensive monitoring capability has many direct benefits to the quality of patient care. Continuous monitoring reduces the time to react to sudden changes in patient condition. In this section, we discuss the potential use of our proposed system to allow a person to detect the early development of liver diseases by performing the tongue diagnosis on the smartphone. Since whether a person has a liver disease can be suggested by bio-markers in the blood sample like elevated ALT/GPT and AST/GOT, we further seek for tongue features to infer the elevation of ALT/GPT and AST/GOT. Then, we can indirectly infer one has liver disease or not by these tongue features. At the same time, these tongue images can be stored in a cloud server for continuous monitoring. People thus can monitor their health instantly and continuously without going to the hospital and reduce the possibility to react to sudden health changes.

There has been a lot of work that used tongue images to analyze or predict disease, including colorectal cancer, Rheumatoid Arthritis (RA), HIV, breast cancer, peptic ulcer disease and liver diseases, etc. In terms of liver diseases, Liu et al. [56] showed that primary liver cancer patients often have blue and purple tongues compared to patients with other cancers. Both primary liver cancer patients and B-virus carriers were found to have this feature, and as the disease progressed, this feature became more prominent [56], [57]. The other studies showed that, as cirrhotic patients developed ascites, tongue furs would almost vanish, and tongue bodies began to shrink and become dry with cracks and red dots [58]. In addition, as the liver healed, tongue fur would become thinner [59] and the colors of tongue furs and tongue body would also change [58].

In order to examine if there is a correlation between some tongue features and the patients' AST/GOT and ALT/GPT, we recruited 246 patients, from April 2014 to December 2016, from health examination center and outpatients of Department of Gastroenterology and Hepatology of Dalin Tzuchi Hospital in Taiwan, including 54 hepatitis patients, 28 cirrhotic patients, 18 liver cancer patients, and 146 patients without liver diseases (verified by blood test and abdominal ultrasound). The study was approved by the Ethics Committee of Dalin Tzu Chi General Hospital (B10401003). Written informed consent was obtained from each patient, and the local Ethics Committee approved the written consent process. The inclusion and exclusion criterion for the subjects is as follows:

- Inclusion criteria

    1. Diagnosed as hepatitis B or C, cirrhosis, and liver cancer by a GI specialist

    2. Patients who had health examination, with blood test and abdominal ultrasound

    3. Patients able to protrude the tongues stably

    4. Patients who had signed IRB agreement.

- Exclusion criteria

    1. Patients unable to stably protrude their tongue.

    2. Patients who had just eaten or drunk something which might color their tongue.

    3. Patients who just did tongue scraping

    4. Cognitive impaired, for example, imbecility dementia or delirium

    5. Patients who had not signed IRB agreement

    6. Patients who didn't have blood test

Nine features including tongue color, tongue size, saliva, tongue fur, tongue fissure, ecchymosis, tooth marks, red dots (and its main area), and sublingual venae were extracted from the tongue image for the analysis. More specifically, each feature is categorized as follows:

    1. Tongue color: slightly white, slightly red, red, dark red

    2. Tongue size: moderate, fat and large

    3. Amount of saliva: little or normal

    4. Tongue fur:

        i.   Color: white, yellow or violet

        ii.   Amount: none, thin, and thick

        iii. Location: spleen-stomach and kidney area, spreading evenly

    5. Tongue fissure: existent or nonexistent

    6. Ecchymosis: existent or nonexistent

    7. Tooth mark: existent or nonexistent

    8. Red dot

        i.   Amount: existent or nonexistent

        ii.   Location: heart-lung area, liver-gall areas, or the others

    9. Sublingual venae: wide and tortuous, otherwise

Each tongue feature variable has two values (present/absent of the feature). On the other hand, the target

variable is the levels of AST/GOT and ALT/GPT in serum and thus contains continuous values. AST/GOT and ALT/GPT are both normally present in serum at a low level. It is reported that normal serum levels are usually less than 40 U/L for AST and less than 50 U/L for ALT. In our analysis, we apply 37 U/L as a common threshold for AST and ALT and use it to discretize them. The serum levels higher than 37 U/L suggests that the patients might have a high risk for liver disease. After discretization, we annotate abnormal and normal for each data instance. Therefore the target variable is converted into binary.

In order to relieve the effect of the small sample size and to find reliable association, we apply three different statistical methods to identify tongue features most related to AST and ALT. First we calculate chi-square statistics between each feature variable and the target variable, and then observe the existence of a relationship between the feature and the target. A p-value less than 0.05 indicates that the tongue feature significantly correlates with the target variable. Maximal information coefficient is the second measure we used for feature selection. It uses a technique that searches for optimal binning and turns mutual information score into a metric that lies in the range [0, 1]. Finally, we apply a robust method of correlation estimation called distance correlation on the dataset. Distance correlation of zero implies that the random variables are statistically independent.

From the three statistical approaches for feature selection, we found the common significant tongue feature variables for AST and ALT respectively. These tongue features and their statistical testing results are shown in Table 8 and Table 9. The number of samples (N) are less than 246 due to that we remove some incomplete data.

Table 8. Tongue features correlated with ALT/GPT

Tongue feature	N	Chi-square			Maximal correlation coefficient	Distance correlation
		value	degree of freedom	p-value		
Tooth mark	235	7.175	1	.007	0.022	.031
Fat tongue	235	4.033	1	.045	0.019	.017

Table 9. Tongue features correlated with AST/GOT

Tongue feature	N	Chi-square			Maximal correlation coefficient	Distance correlation
		value	degree of freedom	p-value		
Thick Fur	232	9.194	1	.002	0.030	0.040
Violet Fur	232	4.137	1	.042	0.011	0.018

We also examine the power of the above features for predicting the levels of AST/ALT by applying a random forest classifier on the dataset. The average accuracy of classification with 10-fold cross validation is about 0.75 for AST and 0.63 for ALT respectively. However, due to the small sample size of our data, the standard deviations are fairly high. We planned to collect more data to develop a reliable and stable prediction model as a future work. Nevertheless, these results clearly suggest the potential of using the smartphone-recorded tongue images to provide an early warning for possible liver disease patient to receive further evaluation of their health conditions.

6. Conclusion and Future work

In this paper, we propose a SVM-based lighting condition estimation method according to color differences of tongue images taken with and without flash on the smartphone under different lighting conditions. We then train a tongue image color correction matrix for each lighting condition based on the ColorChecker to remove the effect of color distortion. The effects of different model parameters and ColorCheckers on the performance of color correction are also discussed. Finally, in order to demonstrate the potential use of our proposed system, we recruited 246 patients and examined the correlations between the captured tongue features and ALT/ AST. We found that some tongue features have strong correlation with the AST or ALT, which suggests the possible use of these tongue features captured on a smartphone to provide an early warning of liver diseases. In the future, we plan to collect more data from different environments, such as different lighting conditions, different smartphones, and more users to validate the usefulness and effectiveness of our proposed system. We would also like to explore more different polynomial models for improving the performance of the color correction matrices.

References

[1]   Zhang, B., Wang, X., You, J., and Zhang, D., Tongue color analysis for medical application. Evid. Based Complement. Alternat. Med. 2013, 2013.

[2]   Zhu, B., Basic theories of traditional Chinese medicine. Published by Singing Dragon, 2010.

[3]   Zhang, H., Wang, K., Zhang, D., Pang, B., Huang, B. Computer aided tongue diagnosis system. The 27th IEEE International Conference of Engineering in Medicine and Biology Society, 2005.

[4]   Kanawong, R., Xu, W., Xu, D., Li, S., Ma, T., and Duan, Y., An automatic tongue detection and segmentation framework for computer-aided tongue image analysis. Int. J. of Functional Informatics and Personalised Medicine. 4(1):56–68, 2012.

[5]   Wang, X., and Zhang, D., A high quality color imaging system for computerized tongue image analysis. Expert Systems with

Applications. 40(15):5854–5866, 2013.

[6]   Kanawong, R., Computer-aided tongue image diagnosis and analysis. University of Missouri at Columbia Columbia, MO, Doctoral
        Dissertation, 2012.

[7]   Lo, L.-C., Cheng, T.-L., Chen, W.-J., Chen, Y.-F., and Chiang, J. Y. The Study on the Agreement between Automatic Tongue
        Diagnosis System and Traditional Chinese Medicine Practitioners. European Congress for Integrative Medicine (ECIM 2012),
        2012.

[8]   Qi WJ, Zhang MM, Wang H, Wen Y, Wang BE, Zhang SW. Research on the relationship between thick greasy tongue fur
        formation and vascular endothelial cell permeability with the protein expression of zonula occludens-1. Chin J Integr Med
        2011;17:510–516.

[9]   Cao MQ, Wu ZZ, Wu WK. Identification of salivary biomarkers in breast cancer patients with thick white or thick yellow tongue
        fur using isobaric tags for relative and absolute quantitative proteomics. J Chin Integr Med / Zhong Xi Yi Jie He Xue Bao. 2011;
        9(3): 275-280.

[10]   Wu Z, Li M, Zhang Y, Chen M. Study on relationship between the thickness of tongue fur and the expressions of apoptosis-related
        genes of the tongue epithelial cells in patients with diseases of the digestive system. J Tradit Chin Med. 2007 Jun;27(2):148-52.

[11]   Li FF, Li GG, Wu YZ, Li J, Zhang XY, Wang HF, Wang YQ. Immunological mechanism of exfoliative tongue fur in children
        with asthma. Zhong Xi Yi Jie He Xue Bao. 2005 Nov;3(6):446-9. Chinese.

[12]   X. Wang, B. Zhang, Z. Yang, H. Wang and D. Zhang, "Statistical Analysis of Tongue Images for Feature Extraction and
        Diagnostics," in IEEE Transactions on Image Processing, vol. 22, no. 12, pp. 5336-5347, Dec. 2013.

[13]   Junwen Zhang, Guangqin Hu and Xinfeng Zhang, "Extraction of tongue feature related to TCM physique based on image
        processing," 2015 12th International Computer Conference on Wavelet Active Media Technology and Information Processing
        (ICCWAMTIP), Chengdu, China, 2015, pp. 251-255.

[14]   Y. C. Hsu, Y. C. Chen, L. c. Lo and J. Y. Chiang, "Automatic tongue feature extraction," Computer Symposium (ICS), 2010
        International, Tainan, 2010, pp. 936-941.

[15]   L. Y. Bai et al., "Automatic extraction of tongue coatings from digital images: A traditional Chinese medicine diagnostic tool," in
        Tsinghua Science and Technology, vol. 14, no. 2, pp. 170-175, April 2009.

[16]   C. W. Huang, Y. J. Chen, T. T. Yen, K. Y. Lin and D. Y. Chen, "Region-based hierarchical tongue feature extraction," 2014
        International Conference on Machine Learning and Cybernetics, Lanzhou, 2014, pp. 867-870.

[17]   Jiatuo Xu, Liping Tu, Zhifeng Zhang, Li Zhang and Changle Zhou, "The region partition of quality and coating for tongue image
        based on color image segmentation method," IT in Medicine and Education, 2008. ITME 2008. IEEE International Symposium
        on, Xiamen, 2008, pp. 817-821.

[18]   C. C. Wei, C. H. Wang and S. W. Huang, "Using threshold method to separate the edge, coating and body of tongue in automatic
        tongue diagnosis," Networked Computing and Advanced Information Management (NCM), 2010 Sixth International Conference
        on, Seoul, 2010, pp. 653-656.

[19]   Y. Wei, J. Li, Q. Chen and M. Liu, "A new pattern recognition algorithm and its application about tongue fur image classification
        of Traditional Chinese Medicine," 2010 3rd International Conference on Biomedical Engineering and
        Informatics, Yantai, 2010, pp. 37-40.

[20]   W. Li, S. Hu, J. Yao and H. Song, "The separation framework of tongue coating and proper in Traditional Chinese Medicine,"
        Information, Communications and Signal Processing, 2009. ICICS 2009. 7th International Conference on, Macau, 2009, pp. 1-4.

[21]   Weitong Huang, Zhaoqian Yan, Jiatuo Xu and Li Zhang, "Analysis of the tongue fur and tongue features by naive Bayesian
        classifier," 2010 International Conference on Computer Application and System Modeling (ICCASM 2010), Taiyuan, 2010, pp.
        V4-304-V4-308.

[22]   K. H. Kim, J. H. Do, H. Ryu and J. Y. Kim, "Tongue diagnosis method for extraction of effective region and classification of
        tongue coating," 2008 First Workshops on Image Processing Theory, Tools and Applications, Sousse, 2008, pp. 1-7.

[23]   X. Li, Q. Shao and J. Wang, "Classification of tongue coating using Gabor and Tamura features on unbalanced data set,"
        Bioinformatics and Biomedicine (BIBM), 2013 IEEE International Conference on, Shanghai, 2013, pp. 108-109.

[24]   R. Kanawong, T. Obafemi-Ajayi, J. Yu, D. Xu, S. Li and Y. Duan, "ZHENG classification in Traditional Chinese Medicine based

on modified specular-free tongue images," Bioinformatics and Biomedicine Workshops (BIBMW), 2012 IEEE International Conference on, Philadelphia, PA, 2012, pp. 288-294.

[25] Bo Huang, D. Zhang, Yanlai Li, Hongzhi Zhang and Naimin Li, "Tongue coating image retrieval," Advanced Computer Control (ICACC), 2011 3rd International Conference on, Harbin, 2011, pp. 292-296.

[26] J. Q. Du, Y. S. Lu, K. Zhang, M. F. Zhu and C. H. Ding, "A Novel Approach of Tongue Body and Tongue Coating Separation Based on FCM," 2nd International Conference on Bioinformatics and Biomedical Engineering, Shanghai, 2008, pp. 2499-2503.

[27] B. Huang, K. Wang, X. Wu, D. Zhang and N. Li, "Quantified Vector Oriented Tongue Color Classification," 2009 2nd International Conference on Biomedical Engineering and Informatics, Tianjin, 2009, pp. 1-4.

[28] SHEN Lan-sun,WANG Ai-min,WEI Bao-guo etc. Image Analysis for Tongue Characterization[J]. Chinese Journal of Electronics, 2001, 29(S1): 1762-1765.

[29] ZHANG Xin-feng, SHEN Lan-sun, WEI Bao-guo, CAI Yi-heng. Application of the Multi-class SVM to the Classification and the Recognition of Tongue Substance and Tongue Coat. Journal of Circuits and Systems《电路与系统学报》2004 年第 5 期 110-113

[30] 王爱民, 赵忠旭, 沈兰荪. 中医舌象自动分析中舌色、苔色分类方法的研究. 北京生物医学工程, 2000, 19(03): 136-142

[31] 李晓宇, 张新峰, 沈兰荪. 基于支撑向量机的中医舌色苔色识别算法研究. 北京生物医学工程, 2006, 25(01): 43-46

[32] 陈海燕, 卜佳俊, 龚一萍, 连奕劭. 一种基于多色彩通道动态阈值的舌苔舌质分离算法. 北京生物医学工程, 2006, 25(5): 466-469

[33] 张静, 张新峰, 王亚真, 蔡轶珩, 胡广芹. 多标记学习在中医舌象分类中的研究. 北京生物医学工程, 2016, 35(2)

[34] 赵荣莱, 许胜, 等. 舌质舌苔的计算机定量描述和分类. 中醫雜誌, 1989；2:47-48

[35] X. Wang and D. Zhang, "An Optimized Tongue Image Color Correction Scheme," in *IEEE Transactions on Information Technology in Biomedicine*, vol. 14, no. 6, pp. 1355-1364, Nov. 2010.

[36] X. Wang and D. Zhang, "A New Tongue Colorchecker Design by Space Representation for Precise Correction," in *IEEE Journal of Biomedical and Health Informatics*, vol. 17, no. 2, pp. 381-391, March 2013.

[37] Hong-Zhi Zhang, Kuan-Quan Wang, Xue-Song Jin and David Zhang, "SVR based color calibration for tongue image," *Machine Learning and Cybernetics, 2005. Proceedings of 2005 International Conference on*, Guangzhou, China, 2005, pp. 5065-5070 Vol. 8.

[38] Cao Meiling, Cai Yiheng, Liu Changjiang and Shen Lansun, "Recent progress in new portable device for tongue image analysis," *Neural Networks and Signal Processing, 2008 International Conference on*, Nanjing, 2008, pp. 488-492.

[39] Jiatuo Xu, Liping Tu, Zhifeng Zhang and X. Qiu, "A medical image color correction method base on supervised color constancy," *IT in Medicine and Education, 2008. ITME 2008. IEEE International Symposium on*, Xiamen, 2008, pp. 673-678.

[40] Yang Cai, "A novel imaging system for tongue inspection," *Instrumentation and Measurement Technology Conference, 2002. IMTC/2002. Proceedings of the 19th IEEE*, 2002, pp. 159-163 vol.1.

[41] L. c. Lo, M. C. c. Hou, Y. l. Chen, J. Y. Chiang and C. c. Hsu, "Automatic Tongue Diagnosis System," *Biomedical Engineering and Informatics, 2009. BMEI '09. 2nd International Conference on*, Tianjin, 2009, pp. 1-5.

[42] Li Zhuo, Jing Zhang, Pei Dong, Yingdi Zhao, Bo Peng, An SA–GA–BP neural network-based color correction algorithm for TCM tongue images, Neurocomputing, Volume 134, 25 June 2014, Pages 111-116

[43] Ini Ryu and Itiro Siio. 2014. TongueDx: a tongue diagnosis for health care on smartphones. In*Proceedings of the 5th Augmented Human International Conference* (AH '14). ACM, New York, NY, USA, , Article 25 , 2 pages

[44] Xu, X., Zhuo, L., Zhang, J., Shen, L. Research on color constancy under open illumination conditions. Journal of Electronics (China). 26(5):681–686, 2009.

[45] Q.H. Su, H. Cheng, W.B. Sun, F.J. Zhang, A novel correction algorithm based on polynomial and TPS models, in: Proceedings of International Conference on Information Technology, Computer Engineering and Management Sciences, 1, 2011. pp. 52–55.

[46] Kim, J., and Scott, C., Variable kernel density estimation. Ann. Stat. 20:1236–1265, 1992.

[47] C.-C. Chang and C.-J. Lin, "LIBSVM: A library for support vector machines," ACM Transactions on Intelligent Systems and Technology (TIST), vol. 2, p. 27, 2011.

[48]   Min-Chun Hu, Ming-Hsun Cheng, Kun-Chan Lan, "Color Correction Parameter Estimation on the Smartphone and Its Application for Automatic Tongue Diagnosis" Journal of Medical Systems, 2015.

[49]   中 医 四 诊 仪 _ 上 海 道 生 中 医 四 诊 仪 _ 中 医 四 诊
http://www.gdzjkf.com/show/b6/78/1_e4_b8_ad_e5_8c_bb_e5_9b_9b_e8_af_8a_e4_bb_aa.htm

[50]   Smith, Thomas; Guild, John (1931–32). "The C.I.E. colorimetric standards and their use". *Transactions of the Optical Society*. **33** (3): 73–134.

[51]   https://en.wikipedia.org/wiki/List_of_color_spaces_and_their_uses

[52]   https://commons.wikimedia.org/wiki/File:CIE1931xy_CIERGB.svg

[53]   Ministry of Health and Welfare. http://www.mohw.gov.tw/cht/DOS/Statistic.aspx?f_list_no=312&fod_list_no=2368 Use URL.

[54]   World Cancer Report 2014. World Health Organization. 2014. pp. Chapter 1.1.

[55]   Jemal, A; Bray, F; Center, MM; Ferlay, J; Ward, E; Forman, D (Mar–Apr 2011). "Global cancer statistics.". CA: a cancer journal for clinicians 61 (2): 69–90. doi:10.3322/caac.20107.

[56]   LIU Qing, YUE Xiao-Qiang, DENG Wei-Zhe, REN Rong-Zhen, Ling Chang-Quan. Quantitative study on tongue color in primary liver cancer patients by analysis system for comprehensive information of tongue diagnosis. Journal of Chinese Integrative Medicine: Volume 1, 2003 Issue 3

[57]   Hsu Lan. Tongue diagnosis of Hepatitis B patients. JOURNAL OF NEW CHINESE MEDICINE November 2013 Vol.45 No.11 P.120-121

[58]   Lee ZH. Atlas for tongue diagnosis, Guangdong publishing house.

[59]   Chen Y, Jiang TH, Ru WZ, Mao AW, Liu Y. Objective tongue inspection on 142 liver cancer patients with damp-heat syndrome. Chin J Integr Med. 2014 Aug;20(8):585-90

[60]   Giannini EG, Testa R, Savarino V. Liver enzyme alteration: a guide for clinicians. CMAJ : Canadian Medical Association Journal. 2005;172(3):367-379. doi:10.1503/cmaj.1040752.